

# Gauge Invariant Implementation of the Abelian Higgs model on Optical Lattices

Yannick Meurice

The University of Iowa

yannick-meurice@uiowa.edu

Work done with Alexei Bazavov, Shailesh Chandrasekharan, Alan Denbleyker, Yuzhi “Louis” Liu, Chen-Yen Lai, Shan-Wen Tsai, Judah Unmuth-Yockey, Tao Xiang, Zhiyuan Xie, Li-Ping Yang, Ji-Feng Yu, Jin Zhang, and Haiyuan Zou

INT, March 26, 2015



# Content of the talk

- Main question: Can we build a Bose-Hubbard quantum simulator for the Abelian Higgs model or its limit the classical  $O(2)$  model with a chemical potential  $\mu$  ?
- The classical lattice Abelian Higgs and  $O(2)$  models
- Tensor RG (TRG) gauge-invariant formulation
- The time continuum limit (connection with the rotor Hamiltonian)
- Finite dimensional projections (quantum link inspired)
- Bose-Hubbard model with 2 species (corresponding to a "spin-1" projection above)
- Optical lattice implementation
- Draft available on request (PRA 90 06303, INT-PUB-15-008, arxiv 1503-xxxx)
- The slides are intended to provide support to the blackboard talk as needed



# Can lattice gauge theorists learn about Quantum Chromodynamics (QCD) at finite density and real time from optical lattice experiments?

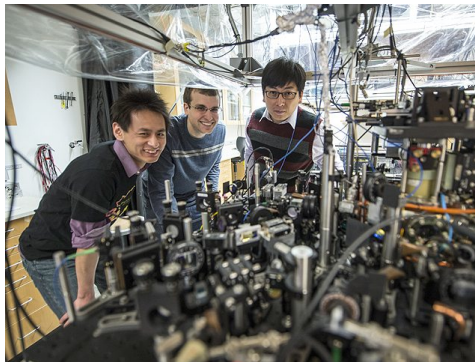


**Figure:** The Fermilab Lattice Gauge Theory cluster (left); An optical lattice experiment in Cheng Chin's lab (right)

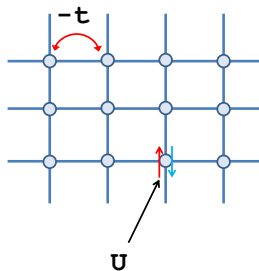


# The Fermi-Hubbard model

Fermi-Hubbard model Hamiltonian:

$$H = -t \sum_{\langle i,j \rangle, \alpha} (c_{i,\alpha}^\dagger c_{j,\alpha} + h.c.) + U \sum_{i=1}^N n_{i\uparrow} n_{i\downarrow}$$

where  $t$  characterizes the tunneling between nearest neighbor sites and  $U$  controls the onsite Coulomb repulsion. These interactions can be approximately recreated with the atoms trapped in an optical lattice.



In the strong coupling limit ( $U \gg t$ ) and at half-filling, Fermi-Hubbard  $\sim$  spin-1/2 quantum Heisenberg

$$H = J \sum_{\langle ij \rangle} \mathbf{S}_i \cdot \mathbf{S}_j \quad \text{with } J = 4t^2/U$$

Using  $\mathbf{S}_i = \frac{1}{2} f_{i\alpha}^\dagger \boldsymbol{\sigma}_{\alpha\beta} f_{i\beta}$ , the Heisenberg Hamiltonian becomes

$$H = \sum_{\langle ij \rangle} -\frac{1}{2} J f_{i\alpha}^\dagger f_{j\alpha} f_{j\beta}^\dagger f_{i\beta} + \sum_{\langle ij \rangle} J \left( \frac{1}{2} n_i - \frac{1}{4} n_i n_j \right)$$

A constraint must be imposed in order to recover the original Heisenberg model:  $f_{i\alpha}^\dagger f_{i\alpha} = 1$ .

The model has a **local**  $SU(2)$  symmetry (Anderson et al.)



# Baryons and Mesons (Fradkin et al.)

After a particle-hole transformation in the spin down operator

$$f_{i,\uparrow}, f_{i,\uparrow}^\dagger \rightarrow \Psi_{x,1}, \Psi_{x,1}^\dagger; \quad f_{i,\downarrow}, f_{i,\downarrow}^\dagger \rightarrow \Psi_{x,2}, \Psi_{x,2}$$

The Heisenberg Hamiltonian can be written as follows

$$H = \frac{J}{8} \sum_{x,\hat{i}} [M_x M_{x+\hat{i}} + 2(B_x^\dagger B_{x+\hat{i}} + B_{x+\hat{i}}^\dagger B_x)] - \frac{Jd}{4} \sum_x (M_x - \frac{1}{2})$$

The “meson” and “baryon” operators are **as in lattice gauge theory**:

$$M_x = \sum_{a=1,2} \Psi_{x,a}^\dagger \Psi_{x,a}$$

and

$$B_x = \sum_{a=1,2} \frac{\epsilon_{ab}}{2} \Psi_{x,a} \Psi_{x,a} = \Psi_{x,1} \Psi_{x,2}$$



# The abelian Higgs model: a feasible first step

- Inexpensive MC simulations at zero density and Euclidean time.
- New Tensor Renormalization Group (TRG) methods (PRD 87 064422 and PRD 89 0160008) allow us to deal with finite density (real chemical potential, complex action) and real continuous time (diagonalization of the transfer matrix).
- Using TRG, we derived a gauge-invariant hopping expansion. We would like to find an optical lattice implementation of this effective action where the gauge fields have been integrated over.
- In a special limit, the model reduces to the  $O(2)$  nonlinear sigma model. We have checked the phase diagram (MI-SF) with the worm algorithm.
- A Bose-Hubbard models with 2 species corresponding to a "spin-1" projection of the  $O(2)$  and Abelian Higgs model with an optical lattice implementation has been proposed (PRA 90 06303 and INT-15-008 arxiv-1503xxxx).
- In the large  $U$  (onsite repulsion) limit, we just obtained a spectrum matching at finite volume (between BH and  $O(2)$  or AbH).



# The Abelian Higgs model on a 1+1 space-time lattice

Fields: a complex (charged) scalar field  $\phi_x$  attached to the sites  $x$  of a space-time lattice and an abelian gauge field

$U_{\langle xy \rangle} = U_{x,\mu} = \exp iA_{\mu}(x)$  attached to the links  $\langle xy \rangle$  with  $y = x + \hat{\mu}$ .

The part of the action  $S$  which corresponds to  $F_{\mu\nu}F^{\mu\nu}$  is obtained by taking products of  $U$ 's around a plaquette  $\mu\nu$  (elementary square in the  $\mu\nu$  plane) denoted  $U_{x,\mu\nu}$ . We use the notation  $\beta_{pl.} = 1/e^2$  and  $\kappa$  for the hopping coefficient. a.k.a. lattice scalar electrodynamics.

$$\begin{aligned} S &= -\beta_{pl.} \sum_x \sum_{\nu < \mu} \text{ReTr} [U_{x,\mu\nu}] + \lambda \sum_x \left( \phi_x^\dagger \phi_x - 1 \right)^2 + \sum_x \phi_x^\dagger \phi_x \\ &- \kappa \sum_x \sum_{\nu=1}^d \left[ e^{\mu ch. \delta(\nu,t)} \phi_x^\dagger U_{x,\nu} \phi_{x+\hat{\nu}} + e^{-\mu ch. \delta(\nu,t)} \phi_{x+\hat{\nu}}^\dagger U_{x,\nu}^\dagger \phi_x \right]. \end{aligned}$$

$$Z = \int D\phi^\dagger D\phi D U e^{-S}$$





# Gauge-invariant effective action

At the lowest order of the strong-coupling expansion we set  $\beta_{pl.} = 0$  (we neglect the plaquette interaction) and carry out the  $DU$  (gauge) integration. The effect of the plaquette can be restored order by order. We obtain an effective theory

$$Z = \int D\phi^\dagger D\phi DU e^{-S} = \int DM e^{-S_{eff.}(M)}$$

for the composite (gauge invariant) field  $M_x = \phi_x^\dagger \phi_x$  with an effective action

$$S_{eff} = \sum_{\langle xy \rangle} (-\kappa^2 M_x M_y + (1/4)\kappa^4 (M_x M_y)^2) \\ - 2\kappa^4 (I_1(\beta_{pl.})/I_0(\beta_{pl.})) \sum_{pl(xyzw)} M_x M_y M_z M_w + O(\kappa^6)$$

Unlike most other approaches we will not try to implement the gauge field on the optical lattice.



# Monte Carlo checks of the hopping expansion and plaquette corrections for $L_\phi = \langle \text{Re}\{\phi_x^\dagger U_{x,\hat{\nu}} \phi_{x+\hat{\nu}}\} \rangle$

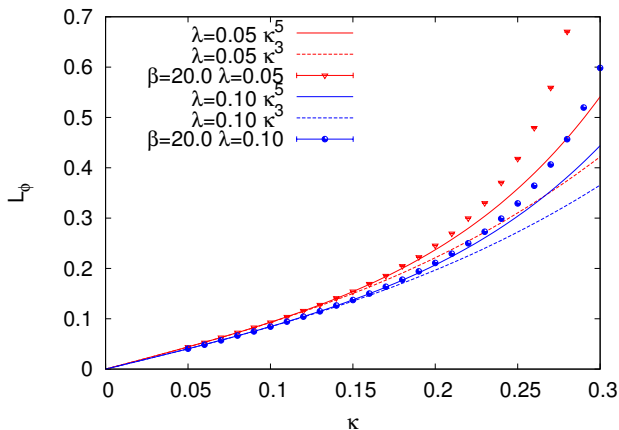
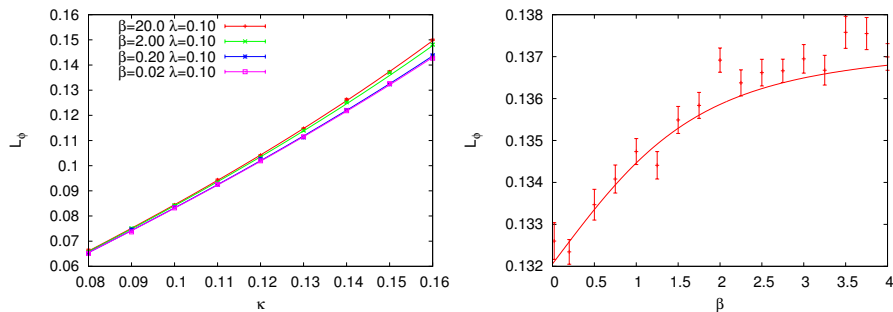


Figure:  $L_\phi$  at  $\beta_{pl} = 20$  for  $\lambda = 0.05$  and  $\lambda = 0.1$  as function of  $\kappa$  compared with the hopping expansion at  $\beta_{pl} = \infty$  at  $O(\kappa^3)$  and  $O(\kappa^5)$ .



# Monte Carlo checks of the hopping expansion



**Figure:**  $L_\phi$  at  $\beta_{pl} = 20, 2, 0.2$  and  $0.02$  for  $\lambda = 0.1$  as function of  $\kappa$  compared with the hopping expansion with included dependence on  $\beta_{pl}$  up to  $O(\kappa^5)$  (left),  $L_\phi$  at fixed  $\kappa = 0.15$  as function of  $\beta_{pl}$  (right).



# The large $\lambda$ limit

We now turn to the limit where  $\lambda$  becomes arbitrarily large. In this limit,  $M_x$  is frozen to 1, or in other words, the Brout-Englert-Higgs mode becomes infinitely massive.

We are then left with compact variables of integration in the original formulation ( $\theta_x$  and  $A_{x,\hat{\nu}}$ ) and the Fourier expansions described before leads to expressions of the partition function in terms of discrete sums. We use the following definitions:

$$t_n(z) \equiv I_n(z)/I_0(z)$$

$$t_n(0) = \delta_{n,0}.$$

For  $z$  non zero and finite, we have  $1 > t_0(z) > t_1(z) > t_2(z) > \dots > 0$   
In addition for sufficiently large  $z$ ,

$$t_n(z) \simeq 1 - n^2/(2z)$$



# Tensor Renormalization Group formulation

As in PRD.88.056005, we attach a  $B^{(\square)}$  tensor to every plaquette

$$= \begin{cases} B_{m_1 m_2 m_3 m_4}^{(\square)} \\ t_{m_{\square}}(\beta_{pl}), & \text{if } m_1 = m_2 = m_3 = m_4 = m_{\square} \\ 0, & \text{otherwise.} \end{cases}$$

a  $A^{(s)}$  tensor to the horizontal links

$$A_{m_{up} m_{down}}^{(s)} = t_{|m_{down} - m_{up}|}(2\kappa_s),$$

and a  $A^{(\tau)}$  tensor to the vertical links

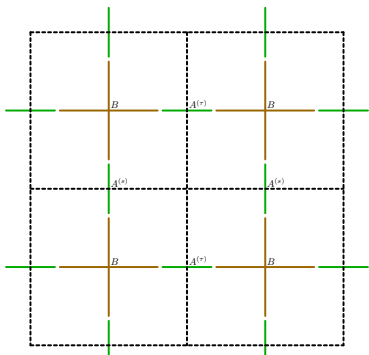
$$A_{m_{left} m_{right}}^{(\tau)} = t_{|m_{left} - m_{right}|}(2\kappa_{\tau}) e^{\mu}.$$



$$Z = \text{Tr}[\prod T]$$

$$Z = (I_0(\beta_{pl}) I_0(2\kappa_s) I_0(2\kappa_\tau))^V \times \text{Tr} \left[ \prod_{h,v,\square} A_{m_{up}m_{down}}^{(s)} A_{m_{right}m_{left}}^{(\tau)} B_{m_1 m_2 m_3 m_4}^{(\square)} \right]. \quad (1)$$

The traces are performed by contracting the indices as shown



The traces can also be expressed in terms of a transfer matrix  $\mathbb{T}$  which can be constructed in the following way.

$$\begin{aligned} \mathbb{B}_{(m_1, m_2, \dots, m_{N_S})}(m'_1, m'_2 \dots m'_{N_S}) &= t_{m_1}(2\kappa_\tau) \delta_{m_1, m'_1} t_{m_1}(\beta_{pl}) \times \\ &t_{|m_1 - m_2|}(2\kappa_\tau) \delta_{m_2, m'_2} t_{m_2}(\beta_{pl}) t_{|m_2 - m_3|}(2\kappa_\tau) \dots \\ &t_{m_{N_S}}(\beta_{pl}) t_{m_{N_S}}(2\kappa_\tau) \end{aligned} \quad (2)$$

Note that with this choice of open boundary conditions, the chemical potential has completely disappeared. If we had chosen different  $m$ 's at the end allowing a total charge  $Q$  inside the interval, we would have an additional factor  $\exp(\mu Q)$ . We next define a matrix  $\mathbb{A}$  as the product.

$$\begin{aligned} \mathbb{A}_{(m_1, m_2, \dots, m_{N_S})}(m'_1, m'_2 \dots m'_{N_S}) &= \\ &t_{|m_1 - m'_1|}(2\kappa_S) t_{|m_2 - m'_2|}(2\kappa_S) \dots t_{|m_{N_S} - m'_{N_S}|}(2\kappa_S) \end{aligned} \quad (3)$$

With these notations we can construct a symmetric transfer matrix  $\mathbb{T}$ . Since  $\mathbb{B}$  is diagonal, real and positive, we can define its square root in an obvious way and write the transfer matrix as

$$\mathbb{T} = \sqrt{\mathbb{B}} \mathbb{A} \sqrt{\mathbb{B}}$$



With this definition, the partition function can be written as

$$Z = (I_0(\beta_{pl}) I_0(2\kappa_s) I_0(2\kappa_\tau))^{V \text{Tr}} \left[ \mathbb{T}^{N_\tau} \right]$$

Alternatively, we could diagonalize the symmetric matrix  $\mathbb{A}$  and define the (dual) transfer matrix

$$\tilde{\mathbb{T}} = \sqrt{\mathbb{A}} \mathbb{B} \sqrt{\mathbb{A}}$$

The  $\mathbb{A}$  and  $\mathbb{B}$  matrices can be constructed by a recursive blocking method similar to those discussed in PhysRevD.88.056005.

$$B'_{m_3 m_6} M(m_1, m_2) M'(m'_1, m'_2) = \tag{4}$$

$$\sum_{m_4, m'_1} B_{m_3 m_4 m_1 m'_1} A^{(\tau)}_{m_4 m_5} B_{m_5 m_6 m_2 m'_2} \tag{5}$$

$$A'_{M(m_1, m_2) M'(m'_1, m'_2)}^{(s)} = A_{m_1 m'_1}^{(s)} A_{m_2 m'_2}^{(s)} \tag{6}$$



# graphical representation of blocking

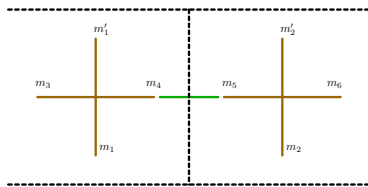


**Figure:** Part of the construction of the blocked  $B'$  tensor. This shows the contraction of the  $B$  and  $A^{(\tau)}$  tensors. The dashed lines are the links of the original lattice.



**Figure:** Graphical representation of the blocking of the  $A$  tensors. The vertical tensors are the  $A^{(s)}$  and the dashed lines are the links of the original lattice.



# The limit $\beta_{pl.} \rightarrow \infty, \lambda \rightarrow \infty$ : the $O(2)$ model

The  $O(2)$  model with one space and one Euclidean time direction. The  $N_x \times N_t$  sites of the lattice are labelled  $(x, t)$ . We assume periodic boundary conditions in space and time.

$$Z = \int \prod_{(x,t)} \frac{d\theta_{(x,t)}}{2\pi} e^{-S} \quad (7)$$

$$S = -\beta_t \sum_{(x,t)} \cos(\theta_{(x,t+1)} - \theta_{(x,t)} + i\mu_{ch.}) \\ - \beta_s \sum_{(x,t)} \cos(\theta_{(x+1,t)} - \theta_{(x,t)}). \quad (8)$$

In the isotropic case, we have  $\beta_s = \beta_t = 2\kappa$ . In the limit  $\beta_t \gg \beta_s$  we reach the time continuum limit.

$\mu_{ch.} \neq 0$ : complex action (no Monte Carlo, but the worm algorithm works well)



# TRG formulation of $O(2)$ with a chemical potential

Using the fact that the Fourier coefficients of  $e^{\beta \cos \theta}$  are  $I_n(\beta)$ , the modified Bessel functions of the first kind, we can write (PRD 89 0160008 and PRA 90 06303)

$$Z = \text{Tr} \prod_{(x,t)} T_{n_x n'_x n_t n'_t}^{(x,t)},$$

with

$$T_{n_x, n'_x, n_t, n'_t}^{(x,t)} = \frac{\sqrt{I_{n_t}(\beta_t) I_{n'_t}(\beta_t) \exp(\mu_{ch.} (n_t + n'_t))}}{\sqrt{I_{n_x}(\beta_s) I_{n'_x}(\beta_s) \delta_{n_x + n_t, n'_x + n'_t}}} \quad (9)$$

Th indices  $n_x$ ,  $n'_x$ ,  $n_t$  and  $n'_t$  label with some abuse of notation the four links coming out of  $(x, t)$  in the  $x$  and  $t$  direction and the trace  $\text{Tr}$  refers to the sum over all these link indices.



# Graphical representation of the blocking process

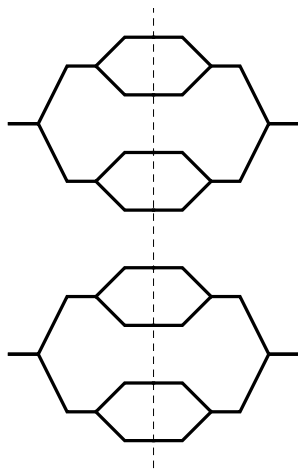


**Figure:** A transfer matrix can be constructed by blocking in the space direction and projecting according the eigenvalues of the tensor norm or the transfer matrix itself.



# Spin-1 projection ( $|n| \leq 1$ , PRA 90 06303)

- If we try to identify the eigenstates of  $L$  with those of the occupation number in the Bose-Hubbard model, we see that the eigenstates are both labeled by integer values. However, in the quantum  $O(2)$  rotor case, the integers are allowed to run from positive to negative values.
- In absence of chemical potential, the negative values can be interpreted as antiparticles
- For a large chemical potential, antiparticles excitations appear as the change in the boson number about some mean background number (MPA Fisher, Sachdev)
- In the following, we consider the quantum link inspired truncation where the original operator algebra is replaced by a finite spin- $s$  representation with  
 $L \rightarrow L^3$ ,  $e^{\pm i\hat{\theta}} \rightarrow L^{\pm}$  and  $|n| \leq s$ . Numerically, we used  $s = 1$ .



# Phase diagram: Mott insulator and Superfluid phases

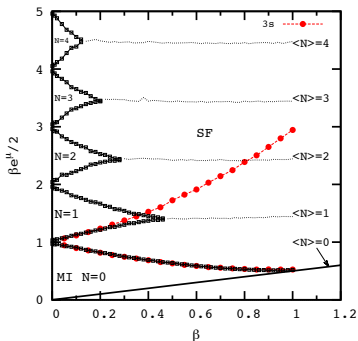
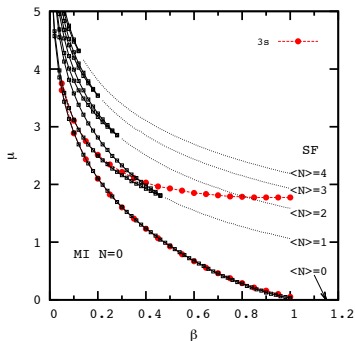


**Figure:** Phase diagram for 2D  $O(2)$  isotropic model in  $\beta$ - $\mu_{ch}$ . plane (left) and in the  $\beta$ - $\beta e^{\mu_{ch}}/2$  plane (right) which resembles the anisotropic case. The lines labeled by "3s" stand for the phase separation lines of a 3-states system



# Remark: N distribution with the TRG and the worm algorithm

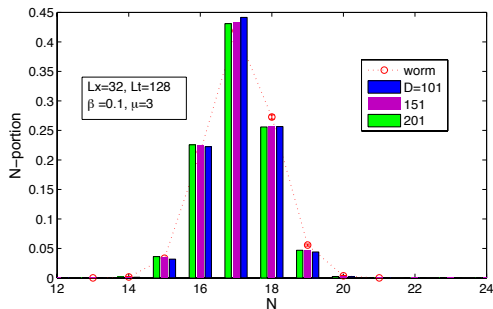


**Figure:** Distribution of  $N = \sum_x n_x$  (conserved charge) calculated with the TRG at 3 truncations and with the worm algorithm (where  $N$  is a winding number). In the large  $L_t$  limit,  $\langle N \rangle$  is quantized. Graph by Li-Ping Yang and Yuzhi Liu.



# Remark: N distribution with the TRG and the worm algorithm: $\mu$ dependence

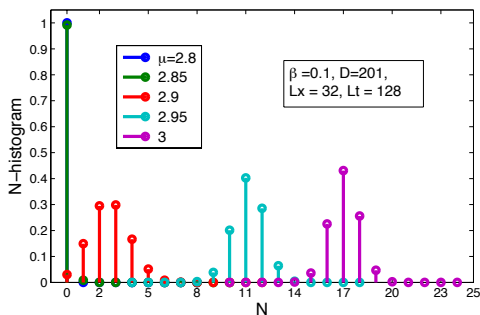


**Figure:** Distribution of  $N = \sum_x n_x$  (conserved charge) calculated with the TRG for increasing  $\mu$ . Graph by Li-Ping Yang.





# Entanglement Entropy as an order parameter

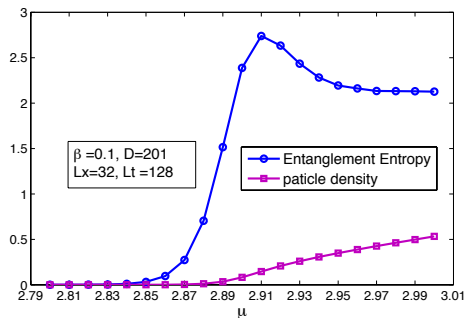


Figure: Graph by Li-Ping Yang



# Time continuum limit

When  $\beta_t \gg \beta_x$  we obtain the time continuum limit (Fradkin, Susskind, Kogut, Polyakov, ..) and a quantum rotor Hamiltonian on a lattice with  $\beta_x$  acting as the coupling between the spatial sites.

$$\hat{H} = \frac{\tilde{U}}{2} \sum_x \hat{L}_x^2 - \tilde{\mu} \sum_x \hat{L}_x - \tilde{J} \sum_{\langle xy \rangle} \cos(\hat{\theta}_x - \hat{\theta}_y), \quad (10)$$

with  $\tilde{U} = 1/(\beta_t a)$ ,  $\tilde{\mu} = \mu_{ch.}/a$  and  $\tilde{J} = \beta_x/a$ , the sum extending over sites  $x$  and nearest neighbors  $\langle xy \rangle$  in space and  $a$  the time lattice spacing.

With the TRG formulation, this limit can be obtained numerically as we keep blocking the transfer matrix in the space direction (coarse graining involving truncations). The spectra in blocks of size 2, 4 and 8 in the spin-1 approximation (we keep only the modes  $n=0$  and  $\pm 1$  at the microscopic level) are shown on the next slide.



# O(2) spectra for L=2, 4, and 8

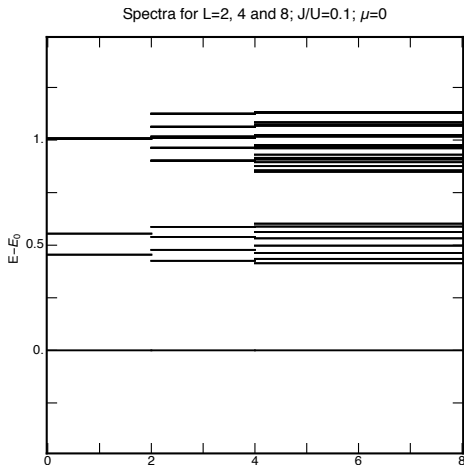


**Figure:** O(2) spectra for L=2, 4, and 8,  $\tilde{J}=0.1$ ,  $\tilde{\mu} = 0$  (Judah Unmuth Yockey). Some higher energy states not shown.



# Two species Bose-Hubbard (PRA 90 06303)

The two-species Bose-Hubbard Hamiltonian ( $\alpha = a, b$  indicates two different species, respectively) on square optical lattice reads

$$\begin{aligned} \mathcal{H} = & - \sum_{\langle ij \rangle} (t_a a_i^\dagger a_j + t_b b_i^\dagger b_j + h.c.) - \sum_{i, \alpha} (\mu + \Delta_\alpha) n_i^\alpha \\ & + \sum_{i, \alpha} \frac{U_\alpha}{2} n_i^\alpha (n_i^\alpha - 1) + W \sum_i n_i^a n_i^b + \sum_{\langle ij \rangle \alpha} V_\alpha n_i^\alpha n_j^\alpha \end{aligned}$$

with  $n_i^a = a_i^\dagger a_i$  and  $n_i^b = b_i^\dagger b_i$ . We impose  $n_i^a + n_i^b = 2$ .

The hopping amplitude is tunable and chosen to be  $t_\alpha = \sqrt{V_\alpha U/2}$ .

The final result is that the effective Hamiltonian at second order in degenerate perturbation theory (Kuklov and Svistunov in 2003) corresponds to the rotor Hamiltonian with

$$\tilde{J} = \sqrt{V_a V_b}, \quad \tilde{U} = 2(U - W), \quad \text{and} \quad \tilde{\mu} = -(\Delta_a - V_a) + (\Delta_b - V_b).$$



# A two species Bose-Hubbard model implementation

In this expression, the chemical potential  $\mu_{a+b}$  is associated with the conservation of  $n^a + n^b$  and should not be confused with the chemical potential introduced in the previous section which couples to  $n^a - n^b$  and breaks the charge conjugation symmetry. In the limit where  $U_a = U_b = U$  and  $W$  and  $\mu_{a+b} = (3/2)U$  much larger than any other energy scale, we have the condition  $n_i^a + n_i^b = 2$  for the low energy sector. The three states  $|2, 0\rangle$ ,  $|1, 1\rangle$  and  $|0, 2\rangle$  satisfy this condition and correspond to the three states of the spin-1 projection considered above.



# Using degenerate perturbation theory

$$\begin{aligned}\mathcal{H}_{\text{eff}} &= \left( \frac{V_a}{2} - \frac{t_a^2}{U_0} + \frac{V_b}{2} - \frac{t_b^2}{U_0} \right) \sum_{\langle ij \rangle} L_i^z L_j^z \\ &+ \frac{-t_a t_b}{U_0} \sum_{\langle ij \rangle} (L_i^+ L_j^- + L_i^- L_j^+) + (U_0 - W) \sum_i (L_i^z)^2 \\ &+ \left[ \left( \frac{pn}{2} V_a + \Delta_a - \frac{p(n+1)t_a^2}{U_0} \right) - \left( \frac{pn}{2} V_b \right. \right. \\ &\left. \left. + \Delta_b - \frac{p(n+1)t_b^2}{U_0} \right) \right] \sum_i L_i^z, \quad (11)\end{aligned}$$

where  $p$  is the number of neighbors and  $n$  is the occupation ( $p = 2$ ,  $n = 2$  in the case under consideration).  $\hat{L}$  is the angular momentum operator in representation  $n/2$ . Matching: with the  $O(2)$  model, we need to tune the hopping amplitude as  $t_\alpha = \sqrt{V_\alpha U/2}$  and have  $\tilde{J} = 4\sqrt{V_a V_b}$ ,  $\tilde{U} = 2(U - W)$ , and  $\tilde{\mu} = -(\Delta_a - V_a) + (\Delta_b - V_b)$ .



# Matching the O(2) and BH spectra for large $U$

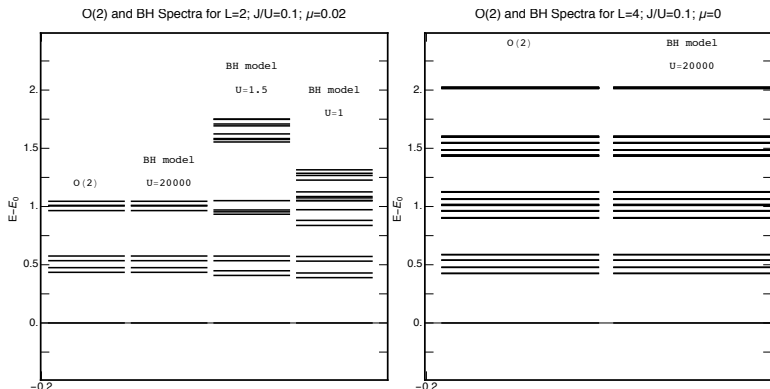


**Figure:** O(2) and Bose-Hubbard spectra for  $L=2$  (left) and  $L=4$  (right) (Jin Zhang and Judah Unmuth Yockey).



# Optical lattice implementation (PRA 90 06303)

- The two-species:  $^{87}\text{Rb}$  and  $^{41}\text{K}$  Bose-Bose mixture where an interspecies Feshbach resonance is accessible
- Due to the physical nature of the different atoms, the hopping amplitudes are different
- Species-dependent optical lattice are used in boson systems, which allows hopping amplitude of individual species to be tuned to desired values.
- The interspecies interaction ( $W$ ) can be controlled by an external magnetic field
- The extended repulsion,  $V_{\alpha}$ , is present and small when we consider Wannier gaussian wave functions sitting on nearby lattice sites (Mazzarella et al. 2006)
- When  $\mu_{ch.}=0$ , it would be desirable to keep the symmetry  $a \leftrightarrow b$  (hyperfine states for the a single type of atoms?). This is a different proposal that we have started investigating





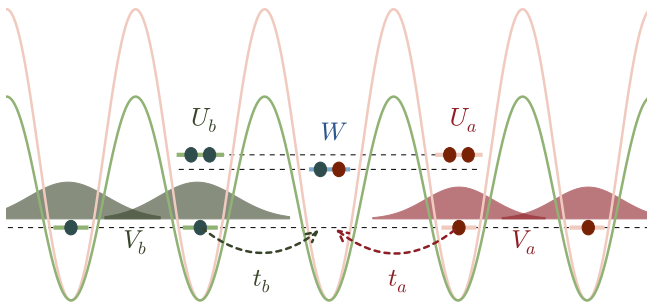


**Figure:** Two-species (green and red) bosons in optical lattice with species-dependent optical lattice (with the same green and red). The nearest neighbor interaction is coming from overlap of Wannier gaussian wave functions. We assume the difference between intra-species interactions are small  $U \gg U - W$ .



# The time continuum limit and the energy spectrum of the Abelian Higgs Model

In the limit  $\kappa_S = 0$ , and if *both*  $\kappa_T$  and  $\beta_{pl}$  become large, at leading order in the inverse of these large parameters, the eigenvalues of  $\mathbb{T}$  are

$$\begin{aligned} \lambda_{(m_1, m_2, \dots, m_{N_s})} = & \\ & 1 - \frac{1}{2} \left[ \left( \frac{1}{\beta_{pl}} (m_1^2 + m_2^2 + \dots + m_{N_s}^2) + \right. \right. \\ & \left. \left. \frac{1}{2\kappa_T} (m_1^2 + (m_2 - m_1)^2 + \dots \right. \right. \\ & \left. \left. \dots + (m_{N_s} - m_{N_s-1})^2 + m_{N_s}^2 \right) \right] \end{aligned}$$

There are two limiting situations:  $1 \ll \beta_{pl} \ll \kappa_T$  and  $1 \ll \kappa_T \ll \beta_{pl}$ .

The second lead to IR problem and we will only consider the case

$1 \ll \beta_{pl} \ll \kappa_T$  and set the scale with the (large) gap energy

$\tilde{U}_g \equiv 1/a\beta_{pl}$ . In addition, we define the (small) energy scales

$\tilde{Y} \equiv (\beta_{pl}/(2\kappa_T))\tilde{U}_g$  and  $\tilde{X} \equiv (\beta_{pl}\kappa_S\sqrt{2})\tilde{U}_g$



$$\partial\mathbb{T}/\partial\kappa_S|_{\kappa_S=0} = (\sqrt{2})(\bar{L}_{(1)}^x + \bar{L}_{(2)}^x)$$

We use the notation  $\bar{L}_{(1)}^x$  to denote the first generator of the spin-1 rotation algebra at the site (1). The notation  $\bar{L}$  is used to emphasize that the spin is related to the  $m$  quantum numbers attached to the plaquettes in contrast to the spin-1 generators  $\hat{L}$  in the  $O(2)$  case having a spin related to the charges  $n$  attached to the time links. The final form of the Hamiltonian  $\bar{H}$  for  $1 \ll \beta_{pl} \ll \kappa_\tau$  is

$$\begin{aligned} \bar{H} = & \frac{\tilde{U}_g}{2} \sum_i (\bar{L}_{(i)}^z)^2 + \\ & \frac{\tilde{Y}}{2} \sum_i (\bar{L}_{(i)}^z - \bar{L}_{(i+1)}^z)^2 - \tilde{X} \sum_i \bar{L}_{(i)}^x. \end{aligned} \quad (12)$$



# A two species Bose-Hubbard model implement ion

For the Hamiltonian  $\bar{H}$  in Eq. (13) corresponding to  $1 \ll \beta_{pl} \ll \kappa_T$ , we need to introduce a new interaction to represent the  $\bar{L}^x$  effects that interchange the  $m = 0$  states with the  $m = \pm 1$  states. This can be achieved by adding the piece

$$\Delta H = -(t_{ab}/2) \sum_i (a_i^\dagger b_i + b_i^\dagger a_i) .$$

The matching between the two models can be achieved by imposing  $t = 0$ ,  $V_a = V_b = -\tilde{Y}/2$  and  $t_{ab} = \tilde{X}$ .

This is a very different realization than for the  $O(2)$  limit. This could be realized with a ladder structure with  $a$  and  $b$  corresponding to the two sides of the ladder. The atoms don't tunnel along the latter but along the rungs to exchange  $a$  and  $b$  at the same rung. The intraspecies interaction  $V$  is attractive, favoring having two atoms in two neighboring sides on the same side of the ladder. This is a ferromagnetic interaction



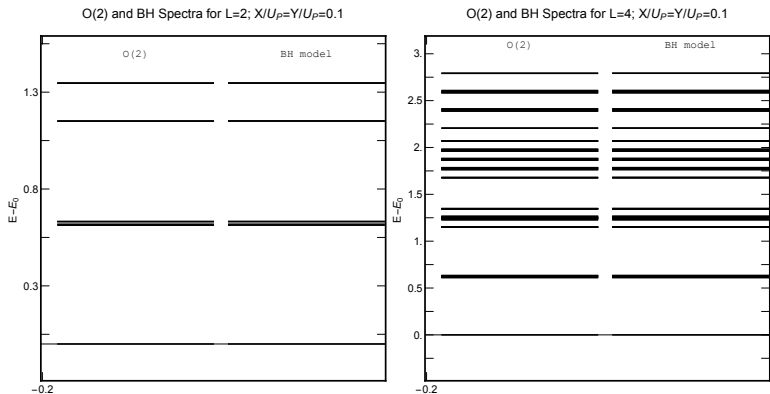


**Figure:** Abelian-Higgs model with  $\tilde{X}/\tilde{U} = 0.1$ ,  $\tilde{Y}/\tilde{U} = 0.1$  and the corresponding Bose-Hubbard spectra for  $L = 2$  (top) and  $L = 4$  (bottom).



# Conclusions

- We proposed a **gauge-invariant** approach for the quantum simulation of the abelian Higgs model.
- Plaquette corrections can be controlled at small hopping.
- The tensor renormalization group formulation allows reliable calculations of the phase diagram and spectrum in the limit  $\lambda \rightarrow \infty$ . The effects of the finite spin projections are small.
- We proposed a Bose-Hubbard model that corresponds to the spin-1 version and proposed an implementation on optical lattices. We were able to **match the spectra in the large  $U$  limit**.
- Different implementations with a manifest symmetry between the two species would be desirable.

This work was supported in part by a DoD contract Award Number W911NF-13-1-0119.

